OPERATIONS AND SUPPLY CHAIN MANAGEMENT
Vol. 19, No. 4, 2026, pp. 640–656
ISSN 1979-3561 | EISSN 2579-9363

A Humanitarian Logistics Model Integrating Heterogeneous Vehicle Routing, Time-Based Transportation Mode Switching, and Overtime Penalties for Disaster Pharmaceutical Logistics

Lingga Ikaditya
Department of Pharmacology and Clinical Pharmacy, School of Pharmacy,
Institut Teknologi Bandung, West Java, Indonesia
Department of Pharmacy, Poltekkes Kemenkes Tasikmalaya, West Java, Indonesia
Email: lingga.ikaditya@gmail.com

Yosi Agustina Hidayat
Industrial Engineering Department, Faculty of Industrial Technology,
Institut Teknologi Bandung, West Java, Indonesia
Email: yosi@itb.ac.id (Corresponding Author)

Zulfan Zazuli
Department of Pharmacology and Clinical Pharmacy, School of Pharmacy,
Institut Teknologi Bandung, West Java, Indonesia
Email: zulfan@itb.ac.id

I Ketut Adnyana
Department of Pharmacology and Clinical Pharmacy, School of Pharmacy,
Institut Teknologi Bandung, West Java, Indonesia
Email: adnyana@itb.ac.id

Zulfian Muhammad Furqon
Industrial Engineering Department, Faculty of Industrial Technology,
Institut Teknologi Bandung, West Java, Indonesia
Email: zulfianfurqon@gmail.com

ABSTRACT

Earthquakes are sudden, unpredictable disasters that disrupt transportation infrastructure while generating surges in medical demand, posing critical challenges to last-mile pharmaceutical logistics. Existing humanitarian logistics models rarely integrate heterogeneous transportation modes, time-dependent mode switching, and operational constraints within a unified framework. This study develops a cost-optimised pharmaceutical distribution model based on a heterogeneous vehicle routing problem (VRP) that incorporates post-disaster infrastructure disruption, time-based mode switching, and overtime penalties. Using the 2022 Cianjur Earthquake (Indonesia) as a case study, three strategies are evaluated: a baseline, a Mixed-Integer Linear Programming (MILP) optimisation model, and a two-phase heuristic combining a savings algorithm with local search. The model distributes 550 pharmaceutical packages to 47 primary healthcare centres (PHCs) under a 480-minute daily operating constraint. The MILP model reduces total cost by 5.89% relative to the baseline (IDR 430,052,945), while the two-phase heuristic achieves the lowest cost (IDR 391,811,960; −8.89%) at a 100% service level. Sensitivity analysis indicates a four-day emergency duration gives the most cost-efficient transition from fast-response modes to consolidated truck distribution. The findings provide a practical optimisation framework and decision-support insights for efficiency, responsiveness, and resilience in disaster pharmaceutical logistics.

Keywords: *pharmaceutical logistics, disaster preparedness, heterogeneous vehicle routing problem (VRP), heuristic optimisation, mode switching, cost efficiency*

1. INTRODUCTION

Earthquakes are highly uncertain natural disasters with extensive destructive impacts, posing a global threat, particularly to countries located along the Pacific Ring of Fire. Approximately 90% of the world's earthquakes occur in this region, placing Indonesia, one of the most seismically active countries, at significant risk (Guha-Sapir & Vos, 2011;

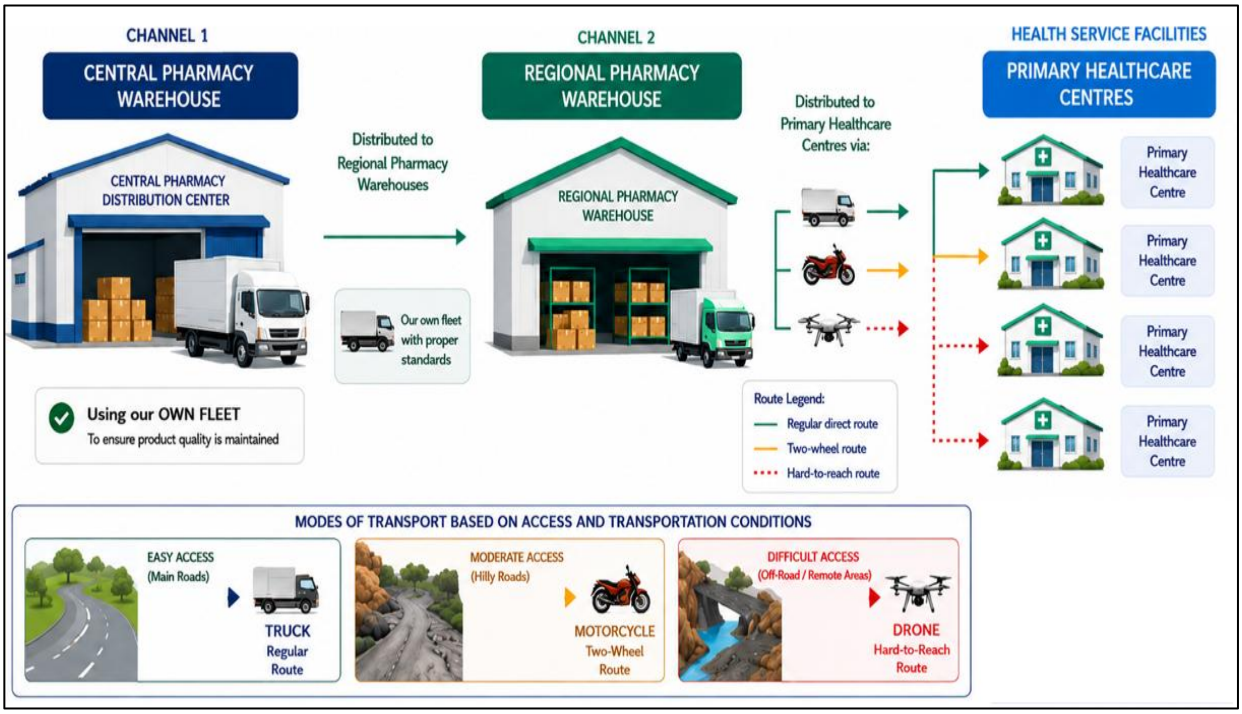

Figure 1 Structural Framework of the Multimodal Medicine Distribution Model

Roque *et al.,* 2024). Such events frequently disrupt transportation systems, healthcare infrastructure, and the supply chains of essential medical commodities, underscoring the strategic importance of effective health logistics during emergency response.

Post-earthquake transportation networks are often severely constrained by debris and infrastructure damage, limiting road accessibility and disrupting multimodal logistics systems (Dukkanci *et al.,* 2023). Rapid restoration is critical to accelerating resource flows and community recovery (Blagojević *et al.,* 2022). Under such conditions, adaptive and time-sensitive transportation strategies are essential to ensure the continuity of emergency supply chains, particularly during the early response period (Mukherji *et al.,* 2014; Zhao *et al.,* 2024).

Disruptions to transportation networks directly affect the timely distribution of medicines and medical equipment. Delays in the delivery of medical aid within the first 12–24 hours have been shown to significantly increase disaster-related mortality (Bobdey, 2012; Shabaninejad *et al.,* 2014). Pharmaceuticals are strategic commodities, and even minor supply chain disruptions can lead to severe health crises (Goodarzian *et al.,* 2020). Distribution systems must therefore be efficient, infrastructure-adaptive, and time-responsive.

Vehicle Routing Problem (VRP)-based approaches have been widely applied in humanitarian logistics optimisation (Goodarzian *et al.,* 2020). However, most existing models assume homogeneous vehicle fleets and stable infrastructure, conditions rarely observed in post-disaster environments. In practice, damaged road networks necessitate the use of heterogeneous transportation modes, including land and aerial vehicles such as trucks, motorcycles, and drones (Dukkanci *et al.,* 2023; Cheng *et al.,* 2024; Chen *et al.,* 2022; Escribano Macias *et al.,* 2020). Despite these developments, integrated models that simultaneously consider heterogeneous fleets, time-based mode switching, and overtime penalties remain limited in the literature.

In Indonesia, a standardised Earthquake Emergency Health Kit (EEHK) comprising 171 essential pharmaceutical and medical items for emergency response has been developed (Ikaditya *et al.,* 2025). While this innovation enhances national pharmaceutical preparedness, the study does not address how EEHK can be distributed efficiently under damaged infrastructure and strict time constraints, revealing a critical gap in disaster pharmaceutical logistics research. Such distribution forms a two-echelon system, emergency supplies move from the National Health Crisis Center Warehouse to a regional depot, then to affected primary healthcare facilities. As routing and allocation decisions occur mainly in the second echelon, this stage is the primary focus of optimisation.

This gap is particularly evident in the context of the 2022 Cianjur Earthquake, where road accessibility evolved dynamically. Several major roads became operational within the first 24 hours, and most road segments were restored within 72 hours, corresponding to the recognised golden rescue period (Ministry of Public Works and Public Housing, 2022; Feng & Wang, 2003). Previous studies have similarly emphasised that early road accessibility is a strategic determinant of effective humanitarian logistics (Sakuraba *et al.,* 2016). Unlike prior studies, this model explicitly integrates time-phased mode switching and labour constraints into a single operational decision framework, which remains largely absent in the humanitarian logistics literature. To address this gap, this study develops an HVRP-based pharmaceutical distribution model (Figure 1). It uses time-based mode switching and overtime penalties as control mechanisms and a dynamic fleet of trucks, motorcycles, and drones in the first 72 hours. The model is demonstrated on the 2022 Cianjur Earthquake.

Table 1 Conceptual Framework of Disaster Logistics Distribution Models

No	Study	Disaster	Transport Modes	Objective	Method	Key Findings	Strengths	Limitations
1	Romero-Mancilla *et al.* (2024)	Earthquake	Truck, van, drone	Cost & time optimisation (3-echelon)	MILP + ε-constraint	Efficient for small–medium cases	Pareto optimal solutions	No motorcycle; Mexico-focused
2	Ma *et al.* (2024)	Earthquake	Road, rail, air	Network resilience evaluation	CMSTAC, logit model	Route-based recovery superior	Strong network focus	Not logistics-delivery oriented
3	(Chen *et al.*, 2022)	Earthquake	Road, rail, air	Cost-efficient interregional logistics	Multi-objective + ACO	Cost-efficient routing	Considers disruption & uncertainty	No small-scale modes
4	(Ramadhan *et al.*, 2025)	Flood	Truck, drone, boat	Multimodal routing optimisation	MILP + RRT	Efficient in urban flooding	Robust matheuristic	Not suitable for mountainous terrain
5	(Shi *et al.*, 2024)	Earthquake /landslide	Truck, drone, helicopter	Emergency scheduling	MIP + heuristic	Suitable for extreme terrain	Multi-modal coverage	No motorcycle integration
6	Dukkanci *et al.* (2023)	Earthquake	Truck, drone	Stochastic routing	Stochastic programming	Handles uncertainty well	Efficient 2-echelon system	Limited transport diversity
7	Cheng *et al.* (2024)	Wildfire	Truck, drone, motorcycle	Collaborative delivery optimisation	LRP + robust optimisation	Effective in constrained areas	Unique multimodal integration	Not earthquake-specific
8	This study	Earthquake	Truck, drone, motorcycle	Adaptive pharmaceutical logistics	MILP + two-phase heuristic	Dynamic routing & improved access	Context-specific & flexible	Limited prior comparable studies

2. LITERATURE REVIEW

Earthquakes are highly destructive events that significantly disrupt healthcare systems and critical infrastructure. Previous studies highlight that earthquakes are among the disasters most severely affecting healthcare facilities, with damage severity increasing alongside seismic intensity (Van Berlaer *et al.,* 2017; Sakarya *et al.,* 2024; Pinzón *et al.,* 2023). Systematic evaluation of damage severity and structural failure is critical (Khanmohammadi *et al.,* 2023). Damaged roads, limited access, and disrupted services hinder timely medical aid, so effective logistics planning is essential for equitable, rapid distribution (Najafi *et al.,* 2013).

Infrastructure networks link supply points to affected populations, so efficient logistics requires targeted, adaptive strategies under disrupted multimodal conditions (Goodarzian *et al.,* 2020; Parker & Maynard, 2015) . However, earthquakes frequently damage transport networks, leading to route failures and delivery delays, which necessitate flexible and resilient logistics systems (Zhao *et al.,* 2024; Dukkanci *et al.,* 2023).

Recent studies have addressed these challenges by integrating multi-depot vehicle routing problems with heterogeneous fleets, enabling adaptive routing under uncertainty and disruption (Ma *et al.,* 2024; Chen *et al.,* 2022). In particular, drones have emerged as a promising solution for last-mile delivery in inaccessible areas, while motorcycles provide flexibility in narrow or damaged roads. Hybrid systems combining trucks, drones, and motorcycles have demonstrated improved efficiency and responsiveness in complex disaster scenarios (Cheng *et al.,* 2024; Romero-Mancilla *et al.,* 2024).

Most humanitarian logistics networks adopt a multi-echelon structure, where large vehicles operate between depots and distribution centres, and smaller modes handle last-mile delivery (Chen *et al.,* 2022). While multimodal integration improves performance, existing studies remain limited in three aspects: (i) insufficient inclusion of flexible small-scale transport such as motorcycles, (ii) lack of focus on pharmaceutical logistics, and (iii) limited consideration of dynamic infrastructure availability in disaster settings. A comparative summary of relevant studies is presented in Table 1 highlighting existing approaches, strengths, and research gaps.

3. METHODOLOGY AND ANALYSIS

This study proposes a MILP model to optimise post-earthquake pharmaceutical distribution, formulated as an integrated location-routing problem accounting for heterogeneous road accessibility, mode capacities, and operational constraints. The distribution network is two-echelon: in the upstream echelon, supplies are shipped from the National Health Crisis Center Warehouse to the Cianjur district pharmaceutical depot; in the downstream echelon, they are distributed from this depot (Cianjur District Health Office) to 47 PHCs. As routing and allocation decisions occur mainly in the second echelon, optimisation focuses on downstream distribution from the depot to the 47 PHCs. Reflecting post-disaster conditions, roads are classified into three levels: fully accessible (trucks), moderately damaged (motorcycles), and severely damaged (drones). The classification derives from BMKG earthquake hazard mapping of the Cugenang Fault (Figure 2), delineating Prohibited (Grey), Restricted (Purple), and Conditional (Blue) zones.

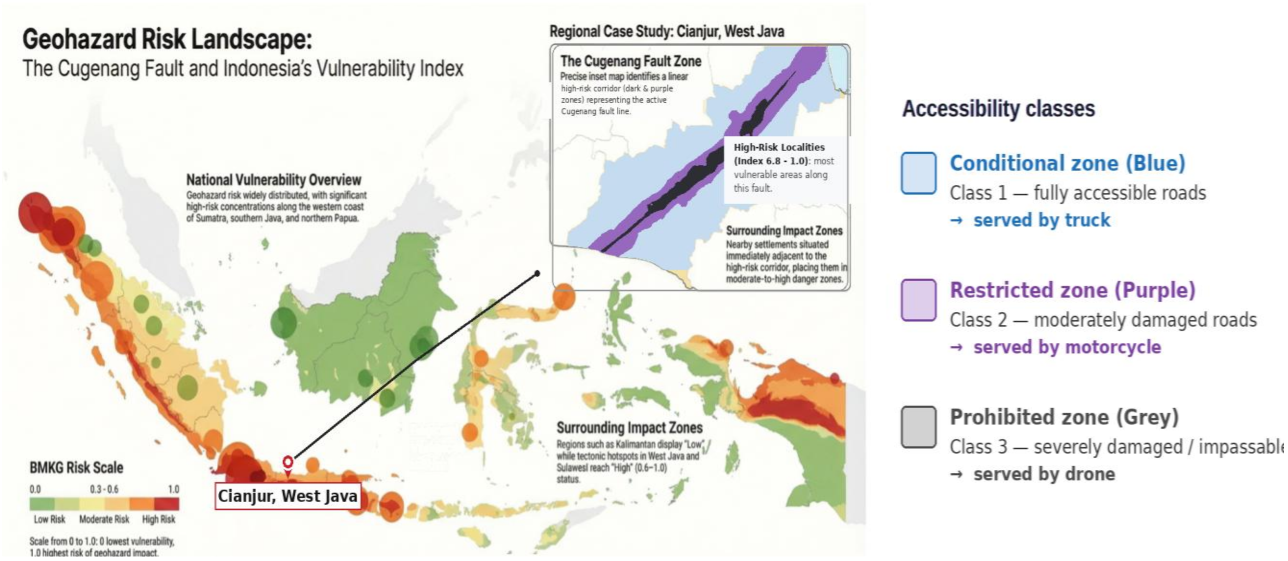

Figure 2 Cianjur Earthquake Hazard Map (Adapted from bmkg.go.id – Earthquake Hazard Map of Cianjur Based on the Cugenang Fault; hazard zones in the inset recoloured to match the accessibility-class scheme)

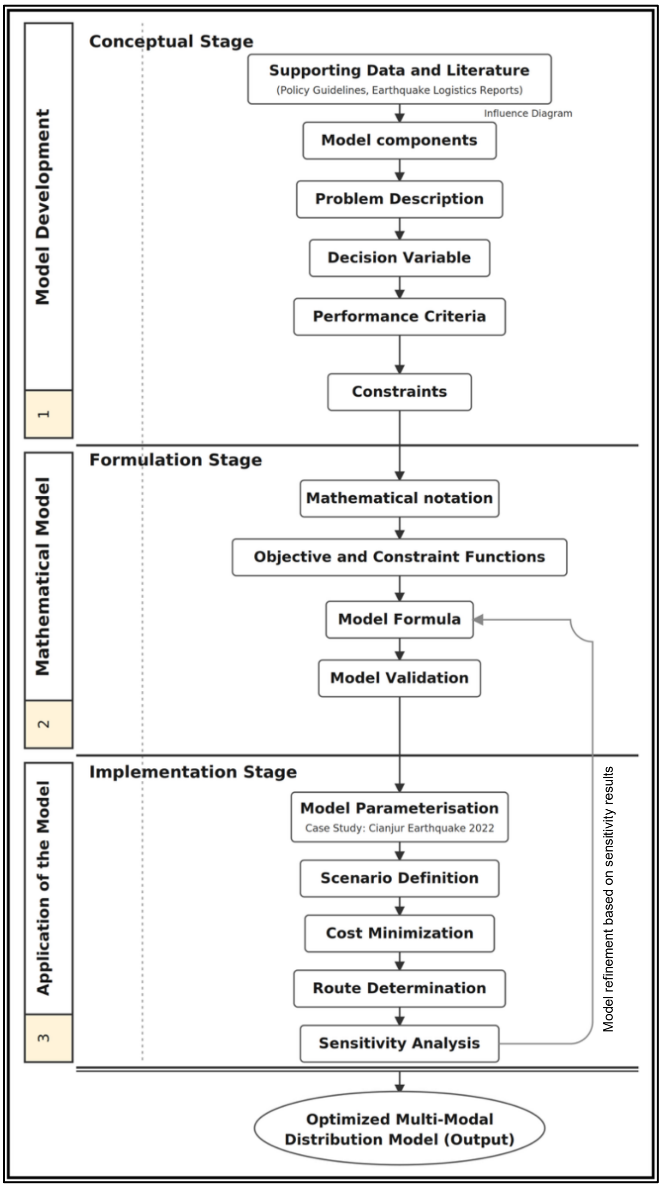

Figure 3 Research Methodology Framework

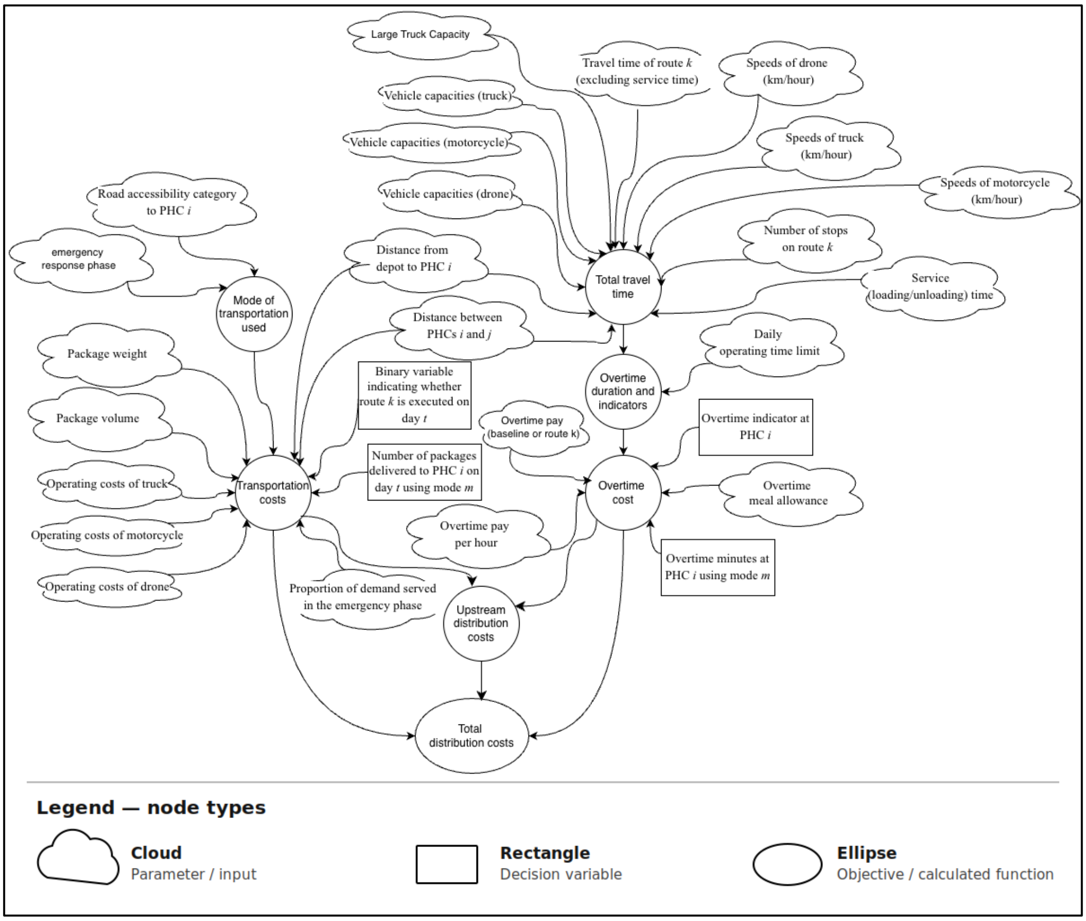

Figure 4 Influence Diagram

The methodological framework integrates mathematical modelling and algorithmic experimentation. Three distribution strategies were evaluated:

(1) A baseline scenario without optimisation;
(2) a savings matrix–based approach to improve routing efficiency through distance and cost reduction; and
(3) a two-phase heuristic combining a savings algorithm, greedy feasibility checks, and local search refinement. The heuristic further incorporated time-based mode switching after 72 hours to represent progressive infrastructure recovery.

The research had three phases (Figure 3). In model development, primary and secondary data (road networks, facility demand, vehicle capacities, response guidelines) were compiled and metrics total cost, delivery time, 72-hour service level defined. In mathematical formulation, the problem was formalised as a MILP model with explicit objectives and constraints, then validated through consistency checks and comparison with heuristic solutions. In model application, it was parameterised with 2022 Cianjur Earthquake data, the three strategies tested, and a sensitivity analysis of emergency-phase duration conducted.

4. MODEL DEVELOPMENT

4.1 Conceptual Model

The conceptual model captures real-world post-disaster conditions from the 2022 Cianjur Earthquake. An influence diagram provides a structured representation of the causal relationships among key variables, illustrating interdependencies between decisions, operational constraints, and performance outcomes within the emergency logistics system.

4.1.1 Model Components

The influence diagram was constructed around the economic objective of minimising total distribution cost. As shown in Figure 4, the model integrates transportation and overtime costs to represent the overall cost structure of pharmaceutical distribution under emergency conditions.

4.1.2 Problem Description

The core problem is minimising total distribution cost, comprising transportation and overtime costs. Transportation cost depends on road accessibility, modes, vehicle operating costs, depot–PHC distances, demand, routing, and shipment quantities. Overtime costs include hourly wages and daily meal allowances, determined by overtime occurrence and duration, which in turn depend on available operating hours and total travel time (a function of speed, distance, service time, capacity, and routing).

4.1.3 Decision Variables

The model has six decision variables for distribution allocation, route selection, and overtime: packages delivered to each PHC per day per mode; binary route-execution decisions; overtime duration at PHCs; overtime indicators at PHCs; route-level overtime duration; and route-level overtime indicators. These are classified as binary (yes–no decisions such as route execution and overtime occurrence) and discrete (quantities such as shipments and overtime durations), distinguishing strategic decisions from numerical allocations.

4.1.4 Performance Criteria

The primary criterion is total distribution cost (the objective function), comprising mode-specific transportation costs, overtime costs from exceeded hours, and meal allowances. Two secondary criteria—total distribution time and service level (proportion of PHC demand fulfilled)—are also considered, so solution quality is evaluated by timeliness and service fulfilment alongside cost. The two cost components are not independent; they interact through a trade-off governed by route consolidation. Consolidating multiple PHCs into one truck route lowers transportation cost by reducing depot round-trips and improving vehicle utilisation, but lengthens route duration; when duration exceeds the 480-minute daily limit (L), the excess is charged as overtime (2 and 4). Decisions that reduce transportation cost thus tend to raise overtime cost, so the two components move in opposite directions with respect to the routing variables. Total cost is therefore quasi-convex in the degree of consolidation, with a minimum at the interior point where the marginal transportation saving from an additional stop equals the marginal overtime penalty. This is confirmed in Table 4, where transportation cost falls while overtime cost rises across Scenarios A–C, and underlies the U-shaped sensitivity curve in Section 5.1.7.

4.1.5 Constraints

Model constraints are defined for three distribution scenarios.

1) Baseline Model. Constraints ensure full demand satisfaction at all PHCs, fix mode selection by road accessibility (trucks for class 1, motorcycles for class 2, drones for class 3), cap daily operating time with optional overtime, and enforce non-negativity and binary overtime indicators.
2) Optimisation Model. Constraints allow demand at motorcycle- or drone-accessible PHCs to be met directly via fast modes or indirectly via consolidated truck routes, and govern candidate-route execution, vehicle-capacity limits on consolidated routes, route-level time feasibility within daily hours (with optional overtime), and non-negativity and binary overtime indicators at the route level.
3) Heuristic Model. Constraints distinguish the emergency phase (≤72 h) from the post-emergency phase (>72 h). In the emergency phase, a portion of demand at motorcycle- or drone-accessible PHCs is served by fast modes; remaining demand is fulfilled post-emergency via consolidated truck routes. Truck-accessible PHCs are served by truck throughout. Vehicle-capacity and route-duration constraints apply, allowing overtime when necessary.

4.2 *Mathematical Model*

Based on the conceptual framework and model components described above, this section presents the formal mathematical formulation of the problem. The formulation includes explicit mathematical notation, an objective function, and constraints for the baseline, optimisation, and heuristic scenarios.

4.2.1 Notation

This section defines the mathematical notation used in the proposed model. Three categories of variables are employed: sets, parameters, and decision variables. Table 2 presents the notations for the data sets used in the model.

Table 2 Notations and Definitions

Notation	Description
P	Set of primary healthcare centers (PHCs)
O	Central pharmaceutical depot
$M = \{T,M,D\}$	Set of transportation modes: truck (T), motorcycle (M), drone (D)
K	Set of candidate truck routes (generated by savings matrix)
$T = \{1,\ldots,H\}$	Set of days (3-month planning horizon)
T_{pre}	Pre-72-hour period (t=1,2,3)
T_{post}	Post-72-hour period (t ≥ 4)
$i, j \in P$	PHC indices
$k \in K$	Candidate route index
$t \in T$	Day index

Based on the problem definition, the following parameters are used.

Parameters:

Pop_i	:	Population in area *i*
q_i	:	Pharmaceutical package demand at PHC *i*
$w_i \in \{1,2,3\}$	:	Road accessibility category to PHC *i*
f_w	:	Mapping function from road class to transportation mode
D_k	:	Total distance of route *k*
d_{ij}	:	Distance between PHCs *i* and *j*
S_{ij}	:	*Saving value*: $d_{oi} + d_{0j} - d_{ij}$
d_{oi}	:	Distance from depot to PHC *i*
n_k	:	Number of stops on route *k*
τ_k	:	Travel time of route *k* (excluding service time)
$\tau_{i,m}^{PP}$	:	Baseline round-trip time to PHC *i* using mode *m*
t_{svc}	:	Service (loading/unloading) time
T_k	:	Total route time
$\alpha_T, \alpha_M, \alpha_D$	:	Travel time per km by mode
L	:	Daily operating time limit (480 minutes)
p_{OT}	:	Overtime wage per hour
p_{meal}	:	Overtime meal allowance
w_{pkg}	:	Package weight
v_{pkg}	:	Package volume
v_t	:	Speeds of truck (km/hour)
v_m	:	Speeds of motorcycle (km/hour)
v_d	:	Speeds of drone (km/hour)
c_t	:	Operating costs of truck (per km)
c_m	:	Operating costs of motorcycle (per km)
c_d	:	Operating costs of drone (per hour)
Q_t	:	Vehicle capacities (truck)
Q_m	:	Vehicle capacities (motorcycle)
Q_d	:	Vehicle capacities (drone)
θ	:	Proportion of demand served in the emergency phase
$\tilde{C}_t, \tilde{C}_m, \tilde{C}_d$	:	Total operating cost of truck, motorcycles and drones
$C_{base}, C_{opt}, C_{heur}$	:	Total operational costs for baseline, optimisation, and heuristic scenarios

Decision Variables:

$x_{i,t}^m$	:	Number of packages delivered to PHC *i* on day *t* using mode *m*
$y_{k,t}$	:	Binary variable indicating whether route *k* is executed on day *t*
$O_{i,t}^m$	:	Overtime minutes at PHC *i* using mode *m*
$z_{i,t}^m$	:	Overtime indicator at PHC *i*
$o_{k,t}$	:	Overtime minutes on route *k*
$z_{k,t}$	:	Route-level overtime indicator

4.2.2 Objective Function and Constraints

The formulation comprises an objective function minimising total distribution cost (transportation and overtime) and constraints governing demand fulfilment, mode accessibility, operating time, vehicle capacity, and mode switching. Equations (1)–(10) define the shared overtime, cost, saving, route-time, and upstream-cost components. For each scenario the objective is presented first, followed by its constraints: baseline objective (11) with constraints (12–15); optimisation objective (16) with (17–21); and heuristic objective (22) with (23–25), where the capacity and route-time constraints (19–21) are shared with the optimisation scenario. All experiments used Gurobi Optimiser v12.0.2 with Python 3.9; configurations, scripts, and dependencies are documented in the supplementary repository for reproducibility.

The distribution network is modelled as a two-echelon system. The upstream echelon covers the deterministic single-truck shipment from the central crisis warehouse to the Cianjur district warehouse, while the downstream echelon covers the optimised distribution to the 47 PHCs. The upstream cost is fixed and identical across all scenarios, and therefore is not subject to optimisation. It enters each objective function as a constant term equal to the upstream cost per EEHK package, IDR 311,260 (Table 3), multiplied by the package demand at each PHC. Because this term takes the same value across scenarios, it shifts all total costs equally and does not affect which solution is optimal. It is retained so that the reported costs reflect the full two-echelon chain, consistent with Indonesian disaster-logistics practice.

$$O_{i,t}^m \geq \tau_i^{PP}(m) - L, O_{i,t}^m \geq 0, O_{i,t}^m \leq M z_{i,t,}^m\ O_{i,t}^m \geq \varepsilon z_{i,t}^m \tag{1}$$

$$O_{k,t} \geq T_k - L, O_{k,t} \geq 0, O_{k,t} \leq M z_{k,t}, O_{k,t} \geq \varepsilon z_{k,t} \tag{2}$$

$$C_{k,t}^{OT} = \left(\frac{O_{k,t}}{60}\right) p_{ot} + p_{meal} \times z_{i,t}^m \tag{3}$$

$$C_{i,t}^{OT} = \left(\frac{O_{k,t}}{60}\right) p_{ot} + p_{meal} \times z_{k,t} \tag{4}$$

$$\tilde{C}_{t,i} = \frac{(2d_{oi}) W_{pkg} c_t}{Q_t} \tag{5}$$

$$\tilde{C}_{m,i} = \frac{(2d_{oi}) c_m}{Q_m} \tag{6}$$

$$\tilde{C}_{d,i} = \frac{\left(\frac{\tau_i^{pp}}{60}\right) c_d}{Q_d} \tag{7}$$

$$S_{ij} = d_{oi} + d_{oj} - d_{ij} \tag{8}$$

$$T_k = \sum_{i \in P} (s_{i,k} \tau_{i,T}^{PP}) + n_k\, t_{svc} \tag{9}$$

$$c_{up} = \frac{C_{trip}^{UP}}{Q_{up}} \tag{10}$$

$$min\, C_{base} = c_{up} \sum_{i \in P} qi + \sum_{t \in T} \sum_{i \in P} \sum_{m \in M} C_{i,t}^m x_{i,t}^m + C_{i,t}^{OT} \tag{11}$$

Constraints:

$$\sum_{t \in T} \sum_{m \in M} x_{i,t}^m = qi, \qquad \forall i \in P \tag{12}$$

$$x_{i,t}^m = 0 \quad jika\ m \neq f(w_i) \tag{13}$$

$$\tau_{i,m}^{PP} \leq L + O_{i,t}^m, \forall i, t,\ \in M \tag{14}$$

$$O_{i,t}^m \geq 0, \quad z_{i,t}^m \in \{0,1\}, \forall i, t,\ \in M\ x_{i,t}^m \geq 0, \forall i, t,\ \in M \tag{15}$$

$$min\, C_{opt} = c_{up} \sum_{i \in P} qi + \sum_{t \in T} \left(\begin{array}{c} \sum_{i:w_i=2} C_{i,t}^M x_{i,t}^M \\ + \sum_{i:w_i=3} C_{i,t}^D x_{i,t}^D + \sum_{k \in K} C_{k,t} y_{k,t} \end{array} \right) + C_{k,t}^{OT} \tag{16}$$

constraints:

$$\sum_{t \in T} \left(x_{i,t}^M + x_{i,t}^D\right) + \sum_{t \in T} \sum_{k \in K} s_{i,k}\ y_{k,t} = q_i, \forall i \in P \tag{17}$$

$$y_{k,t} \in \{0,1\}, \forall k \in K,\ t \in T \tag{18}$$

$$\sum_{i \in P} q_i\ s_{i,k} \leq Q^T, \forall k \in K \tag{19}$$

$$T_k \leq L + o_{k,t}, \forall k \in K,\ t \in T \tag{20}$$

$$o_{k,t} \geq 0, \quad z_{k,t} \in \{0,1\}, \forall k, t \tag{21}$$

$$\min C_{heur} = c_{up} \sum_{i \in P} qi + \sum_{t \in T_{pre}} \Big(\sum_{i:w_i=2} C_{i,t}^M x_{i,t}^M + \sum_{i:w_i=3} C_{i,t}^D x_{i,t}^D + \sum_{k \in K} C_{k,t} y_{k,t}\Big) + \sum_{t \in T_{post}} \sum_{k \in K} C_{k,t} y_{k,t} + C_{k,t}^{OT} \tag{22}$$

constraints:

$$\sum_{t \in T_{pre}} \left(x_{i,t}^M + x_{i,t}^D\right) = \theta\, q_i, \forall i\colon w_i \in \{1,2,3\} \tag{23}$$

$$\sum_{t \in T_{post}} \sum_{k \in K} s_{i,k}\ y_{k,t} = (1-\theta)\, q_i, \forall i\colon w_i \in \{2,3\} \tag{24}$$

$$\sum_{t \in T} \sum_{k \in K} s_{i,k}\ y_{k,t} = q_i, \forall i\colon w_i = 1 \tag{25}$$

Constraints (1) and (2) ensure each mode operates at most 480 minutes per day at the point and route levels, respectively; excess round-trip time is recorded as overtime. Overtime cost combines hourly overtime duration and a daily meal allowance, defined for point-level deliveries in (3) and consolidated truck routes in (4).

Distribution costs are formulated in (5)–(7). Truck cost is the round-trip depot–PHC distance times package weight and truck cost per km per ton (5). Motorcycles and drones need multiple trips per demand point: motorcycle cost is round-trip distance times 16 units per package and cost per km (6); drone cost divides total drone travel time by 60 (minutes to hours), times 35 trips per package and hourly operating cost (7).

The route-saving method builds a saving matrix in which the saving value (8) evaluates consolidation efficiency under the 480-minute daily limit. Candidate truck routes and their total travel time are given in (9), and (10) computes the

Table 3 Parameter Values Used in the Experiments

No	Parameter	Value	Unit/Source
1	c_t	577.08	IDR per km per ton (truck)(Ministry of Transportation RI, 2019)
2	c_m	385.66	IDR per km (motorcycle)
3	c_d	20,304	IDR per hour (drone)(Rahadian, 2020)
4	w_{pkg}	2.359	Ton per package
5	v_{pkg}	7.52	m^3
6	L	480	Daily operating limit (minutes)
7	p_{OT}	13,000	Overtime wage (IDR/hour)
8	p_{meal}	30,000	Meal allowance per overtime day (IDR)
9	t_{svc}	60	Service time per stop (minutes)
10	v_t	30	Truck speed (km/h)
11	v_m	15	Motorcycle speed (km/h)
12	v_d	40	Drone speed (km/h)
13	Q_t	1	Truck capacity (package)
14	Q_m	1/16	Motorcycle capacity (package)
15	Q_d	1/35	Drone capacity (package)
16	θ	0.033	Proportion of total pharmaceutical demand required during the emergency response phase, estimated using a time-based allocation approach (3-day emergency period / 90-day planning horizon).
17	c_{up}^{trip}	1,245,038	Truck transportation cost per trip from the National Health Crisis Center Warehouse to the District Pharmaceutical Warehouse (IDR)
18	Q_{up}	4	Truck capacity (packages) from the National Health Crisis Center Warehouse to the District Pharmaceutical Warehouse
19	c_{up}	311,260	Transportation cost per EEHK package from the National Health Crisis Center Warehouse to the District Pharmaceutical Warehouse (IDR/package)

per-parcel upstream cost from the Central Crisis Warehouse to the District Warehouse, included in all objective functions.

In the baseline (objective 11), total cost—truck (with overtime), motorcycle, and drone—is minimised without consolidation, so services are direct via the feasible mode. Constraints require full demand satisfaction over the 90-day horizon (12); (13) assigns each mode by road class (1: truck, 2: motorcycle, 3: drone), restricting switching; (14) caps round-trip time at 480 minutes unless compensated by overtime; and (15) enforces non-negative overtime with binary indicators and non-negative quantities.

In the optimisation scenario (objective 16), total cost is minimised while accounting for consolidation from the saving matrix. Constraints satisfy class-2/3 PHC demand by motorcycle/drone and/or trucks on consolidated routes k (17); (18) determines route execution; (19) limits packages to route capacity; (20) caps route duration at 480 minutes unless overtime applies; and (21) sets non-negative overtime with binary indicators.

In the heuristic scenario (objective 22), total cost is minimised under consolidation with mode switching after 72 hours, as motorcycle/drone services shift to trucks with improving roads. Constraints require a proportion (θ) of truk/motorcycle/drone-accessible demand served by fast modes in the first 72 hours (23); the remaining (1−θ) reassigned to consolidated truck routes post-72-hour (24); and class-1 PHCs served by truck throughout (25). Capacity and route-time constraints are identical to the optimisation scenario (19) – (21).

4.2.3 Model Verification

The model was verified for logical consistency through dimensional-consistency checks across equations and boundary tests, confirming that the formulation behaves as intended before computational experiments.

5. RESULTS AND DISCUSSION

5.1 Application of the Model

This section presents the parameterisation and computational experiments evaluating the approach under three scenarios: (A) baseline, (B) optimisation, and (C) two-phase heuristic.

5.1.1 Parameterisation

Table 3 summarises the experimental parameters, obtained from relevant references and, where necessary, derived through intermediate calculations.

Vehicle operating costs were computed from the round-trip depot–PHC distance. Demand at each PHC was estimated from its service population, assuming one package per 1,000 residents over a 90-day horizon. Each package weighs 2.359 tons and occupies 7.52 m³, constraining feasibility; a truck carries one package per trip, motorcycles and drones 1/16 and 1/35 of a package per trip. Mode-specific costs follow (5) – (7).

Truck:

$$\tilde{C}_{t,i} = \frac{(2d_{oi})W_{pkg}c_t}{Q_t} \tag{5}$$

Table 4 Comparison of Cost Components, Service Level, and Total Cost Across Scenarios.

No	Scenario	Total Routes	Total Packages	Service Level (%)	Truck Cost (IDR)	Motorcycle Cost (IDR)	Drone Cost (IDR)	Transportation Cost (Subtotal)	Overtime Cost (IDR)	Total Cost (IDR)
1	A	47	550	100	145,314,230	77,916,292	30,891,224	254,121,746	4,738,199	430,052,945
2	B	24	550	100	118,572,769	77,916,292	30,891,224	227,380,285	6,150,250	404,723,535
3	C_Pre72	23	69	100	5,221,971	986,004	3,952,898	10,160,873	135,400	10,296,273
	C_Post72	24	481	100	195,992,360	-	-	195,992,360	14,330,327	210,322,687
	C_(Total)	23+24	550	100	201,214,331	986,004	3,952,898	206,153,233	14,465,727	391,811,960

The Transportation Cost (Subtotal) column reports downstream costs only (truck + motorcycle + drone) and equals the sum of the three mode columns. The fixed upstream cost (IDR 171,193,000, central crisis warehouse to Cianjur district warehouse) is invariant and added once in Total Cost. Thus, Total Cost = Transportation Subtotal + Overtime + Upstream for full-horizon rows (A, B, C Total), while the C Pre- and Post-72-hour rows decompose downstream cost only, the upstream constant added once in C (Total).

Motorcycle:

$$\tilde{C}_{m,i} = \frac{(2d_{oi})c_m}{Q_m} \tag{6}$$

Drone:

$$\tilde{C}_{d,i} = \frac{\left(\frac{\tau_i^{pp}}{60}\right)c_d}{Q_d} \tag{7}$$

Overtime costs arise when daily operating time exceeds 480 minutes, mainly for trucks serving remote PHCs. Motorcycles and drones are constrained by daily fleet availability (16 motorcycles/day and 35 drones/day) and do not generate overtime in the baseline. Overtime cost combines hourly wages and a daily meal allowance, computed as:

$$C_{k,t}^{OT} = (\frac{O_{k,t}}{60})p_{ot} + p_{meal} \times z_{k,t} \tag{4}$$

5.1.2 Comparative Performance of Distribution Scenarios

Comparing Scenarios A, B, and C shows a clear progression in cost efficiency as decision integration increases. As summarised in Table 4 (comparison of total cost across scenarios). Scenario A has the highest cost (IDR 430,052,945), reflecting inefficient routing without consolidation consistent with findings that uncoordinated routing yields duplicated trips and low utilisation (Balcik & Beamon, 2008; Wohlgemuth *et al.,* 2012).

The improvement in Scenario B, where routes decrease from 47 to 24, confirms the role of consolidation in routing efficiency: combining multiple service points into fewer trips reduces redundant travel and improves vehicle utilisation, lowering transportation cost and total cost by approximately 5.89%. This is consistent with studies identifying route consolidation as a key mechanism for operational efficiency in vehicle routing problems (Wohlgemuth *et al.,* 2012).

Scenario C achieves the lowest cost (IDR 391,811,960; −8.89%) via a time-based adaptive strategy: higher pre-72-hour cost is offset by post-72-hour savings, showing efficiency depends not only on route optimisation but on aligning modes with evolving infrastructure building on Balcik and Beamon (2008) on phase-dependent humanitarian operations.

Disaggregated analysis (Table 4) shows key trade-offs. Scenario A has high transportation cost with minimal overtime (inefficient). Scenario B cuts transportation cost via consolidation but raises overtime from longer routes—a cost-versus-intensity trade-off. Scenario C further cuts transportation cost while substantially increasing overtime, yet attains the lowest total cost, indicating controlled overtime is economically justified; consistent with disaster-logistics studies (Balcik & Beamon, 2008), it reflects necessary operational intensification, not inefficiency.

5.1.3 Routing Structure and Trip Efficiency

The comparison of routing structures reveals a clear shift in trip organisation across scenarios. The route reduction achieved by Scenario B (Section 5.1.2) provides empirical support for the role of minimising redundant trips in improving routing efficiency, consistent with humanitarian vehicle-routing studies showing that coordinated strategies reduce trip duplication and improve vehicle utilisation (Wohlgemuth *et al.,* 2012), and with multimodal-routing research demonstrating that integrating transport modes reduces redundant trips (Masmoudi *et al.,* 2022). In the present study these gains are further reflected in lower total distribution costs through time-dependent mode switching. Scenario C, however, presents a different pattern: being phase-dependent (23 routes pre-72-hour and 24 post-72-hour), it shows that a lower route count does not necessarily imply higher efficiency. Instead, efficiency arises from the interaction between consolidation and the temporal structuring of trips: by distributing trips across phases and aligning modes with infrastructure conditions, Scenario C attains superior cost performance despite more routes. This is consistent with recent emergency-logistics studies in which truck–drone coordination and hybrid heuristics improve routing efficiency and solution quality (Weng *et al.,* 2024).

Routing efficiency should therefore be judged not by route reduction alone but by how trips are organised and coordinated over time. Time-dependent vehicle-routing research shows that travel times, operational costs, and service conditions vary dynamically across periods, shaping routing decisions and system performance (Luo *et al.,* 2023; Menares *et al.,* 2023). In particular, Luo *et al.* (2023) shows that time-dependent travel speeds significantly affect route selection and cost optimisation, highlighting the importance of incorporating temporal variability into routing models. Similarly, Menares *et al.* (2023) add that service conditions and failure probabilities are likewise time-dependent. In disaster pharmaceutical logistics this variability extends beyond traffic to evolving infrastructure accessibility, so routing efficiency emerges from the coordinated interaction of consolidation and time-dependent mode selection, as Scenario C illustrates.

To illustrate consolidation's effect on response time and cost, Table 5 compares routing before and after consolidation for a representative northern cluster (P20, P22, P23, P34). Before, each PHC is served by an independent depot round-trip (four routes); after, these merge into one multi-stop truck

Table 5 Comparison of Routes Before and After Consolidation (Illustrative Northern-Cluster Example)

Metric	Before (4 Direct Trips)	After (1 Consolidated Route)
Number of Routes/Trips	4 separate depot round-trips	1 multi-stop route
PHCs Served	P20, P22, P23, P34 (separately)	P20–P22–P23–P34 (single route)
Route Duration	4 independent round-trips	400 min (160 travel + 240 service)
Within 480-min Limit?	Yes (each trip)	Yes — no overtime triggered
Vehicle Capacity Utilisation	Low (one demand point per trip)	High (load aggregated over 4 stops)
Effect on Transportation Cost	Higher (redundant depot travel)	Lower (redundant travel removed)

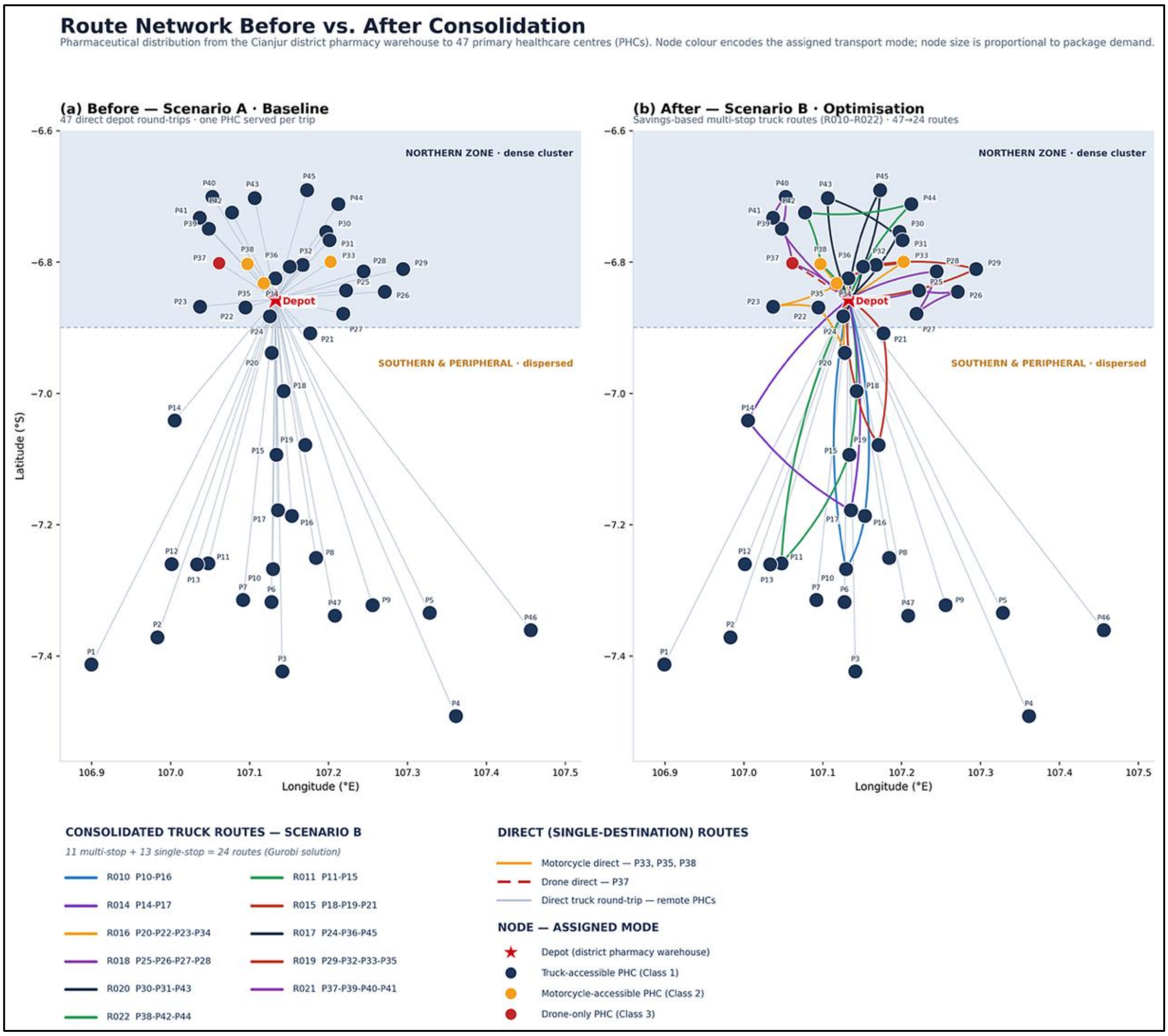

Figure 5 Route Network Before (Scenario A, 47 Routes) vs. After Consolidation (Scenario B, 24 Routes)

route of about 80 km—160 minutes of travel plus 240 minutes of service (4 × 60), totalling 400 minutes, within the 480-minute limit, so no overtime is triggered. Aggregated across all PHCs, this reduces the active route count from 47 (Scenario A) to 24 (Scenario B) and lowers total cost from IDR 430,052,945 to IDR 404,723,535 (−5.89%).

5.1.4 Spatial Configuration and Routing Strategy

The spatial configuration of distribution reflects the interaction between road-accessibility zones and the savings-based routing structure. Figure 5 shows the assignment of transport modes to each PHC according to the BMKG hazard classification: trucks serve fully accessible (class 1) roads, motorcycles serve moderately damaged (class 2) roads, and drones serve severely damaged (class 3) roads, with node sizes scaled to package demand. The corresponding route network, generated using the Clarke–Wright savings algorithm, is shown in Figure 5b, where two dominant routing patterns can be identified. First, clustered multi-stop routes emerge in areas with high densities of healthcare facilities and relatively short inter-facility distances, thereby enhancing vehicle utilisation and reducing overall travel costs. This pattern is particularly observable in the northern region, where multiple PHCs are consolidated into interconnected truck routes over short distances. This pattern is consistent with established vehicle routing principles, whereby savings-based heuristics facilitate efficient route consolidation (Laporte, 2009; Golden *et al.,* 2008).

Second, direct routes are predominantly assigned to remote or geographically isolated primary healthcare centres (PHCs), where accessibility constraints and urgency necessitate prioritising delivery timeliness over consolidation efficiency. This is reflected in the long, radial routes extending towards the southern and peripheral areas in Figure 5, indicating direct connections from the depot to isolated PHCs. This finding aligns with prior studies in humanitarian logistics, which emphasise that minimising response time is critical to reducing human suffering in disaster contexts. Consequently, direct delivery strategies are often required to minimise response delays, particularly in disaster-affected and hard-to-reach areas (Balcik & Beamon, 2008; Holguín-Veras *et al.,* 2013).

The prevalence of direct, single-destination routes in the southern and peripheral areas is a direct consequence of the vehicle capacity constraint (19) and the 480-minute route-duration limit (20), rather than an absence of routing decisions. Each pharmaceutical package weighs 2.359 tons and occupies 7.52 m³ (Table 3), and a single truck carries one package per trip; a consolidated route is feasible only when the combined load of its stop's respects vehicle capacity and the combined duration respect the daily operating limit. For isolated PHCs, a single round-trip already approaches the daily time budget once the 60-minute service time per stop is included, leaving no feasible slack to append additional stops without incurring substantial overtime. Consequently, the savings algorithm retains these locations as direct routes. Such routes exhibit lower vehicle capacity utilisation than consolidated multi-stop routes, because the vehicle returns to the depot after serving a single demand point. This represents a deliberate trade-off: where geographic dispersion makes consolidation infeasible, the model accepts reduced utilisation to preserve delivery feasibility and responsiveness. In contrast, the dense northern cluster permits multi-stop consolidation over short inter-facility distances, yielding markedly higher utilisation. This pattern explains why route reduction in the optimisation scenario (from 47 to 24 routes) is concentrated in the northern cluster, while southern PHCs remain served by direct routes.

5.1.5 Cross-Scenario Routing Logic

The route counts across all scenarios follow directly from the savings-based construction of candidate truck routes rather than from any preset value. The Clarke–Wright algorithm initialises with n = |P| separate routes, each serving one demand point (Clarke & Wright, 1964; Laporte, 2009)—mathematically equivalent to the baseline (47 PHCs, 47 direct round-trips). It then computes the saving value $S_{ij}=d_{oi}+d_{oj}-d_{ij}$ for every pair (Eq. 8), sorts these values in descending order, and merges routes only while the capacity (Eq. 19) and route-duration (Eq. 20) constraints remain satisfied; otherwise, the pair is skipped. The final route count is thus an emergent outcome of how many merges are feasible.

Scenario B applies full consolidation, reducing the 47 baseline trips to 24 routes (11 multi-stop and 13 single-stop). The efficiency gain arises through two mechanisms: improved capacity utilisation, with the mean number of stops per route rising from 1.00 in Scenario A to 1.96 in Scenario B, and reduced aggregate travel distance, as depot–point–depot segments are replaced by shorter inter-facility legs (Laporte, 2009). Together these lower truck transportation cost by 18.4% and yield the 5.89% total-cost reduction. Consolidation simultaneously raises overtime from IDR 4.7 million (A) to IDR 6.2 million (B), but the transportation saving far exceeds this increase, consistent with the quasi-convex cost structure described in Section 4.1.4.

Scenario C adds time-based mode switching to Scenario B's consolidated structure; the two differ in their phase-dependent mode schedule, not in their underlying route set. In the pre-72-hour phase, four access-constrained PHCs (P33, P35, and P38 by motorcycle, P37 by drone) are served individually by fast modes while the remaining PHCs already operate on consolidated truck routes, giving 23 active routes. Once roads recover within the golden period, these four PHCs switch to truck after 72 hours and the network reverts to Scenario B's 24-route structure (Table 6). The most heavily used consolidated truck routes after the transition are summarised in Table 7. The additional saving in Scenario C (8.89% versus 5.89%) therefore originates from substituting cheaper modes early in the response, not from adding or removing routes, consistent with phased disaster-response models in which early operations prioritise speed and later phases emphasise cost (Balcik & Beamon, 2008; Holguín-Veras *et al.,* 2013).

A notable structural finding is that Scenario C and Scenario A share the same total route count of 47, yet the equality is not coincidental and does not imply identical routing. In Scenario A, all 47 routes are independent single-destination depot round-trips (depot – one PHC – depot) operating with a fixed mode and a static schedule over the entire 90-day horizon. In Scenario C, the 47 routes are distributed across two temporal phases (23 pre-72-hour plus 24 post-72-hour; Table 4): the pre-72-hour routes are direct single-destination trips by fast modes that temporarily reverse Scenario B's consolidation to prioritise responsiveness, while the 24 post-72-hour routes are consolidated multi-stop truck routes identical in construction to those of Scenario B. Scenario C is thus a dynamic, two-phase strategy incorporating time-based mode switching that is entirely absent from the static baseline, consistent with phased disaster-response frameworks that separate a responsiveness-oriented relief phase from an efficiency-oriented recovery phase (Balcik & Beamon, 2008; Holguín-Veras *et al.,* 2013).

The two scenarios therefore differ fundamentally in cost and responsiveness despite their identical route count: Scenario C attains the lowest total cost (IDR 391,811,960; −8.89% relative to baseline) because efficiency is gained through temporal phasing and mode adaptation rather than route reduction alone. Had the route structures been identical, the total costs would coincide. This indicates that, in disaster pharmaceutical logistics, the route count alone is not a reliable proxy for system performance; the organisation and timing of trips matter more than their absolute number—a view echoed in time-dependent routing research where temporal coordination, not trip count, drives efficiency (Luo *et al.,* 2023; Menares *et al.,* 2023).

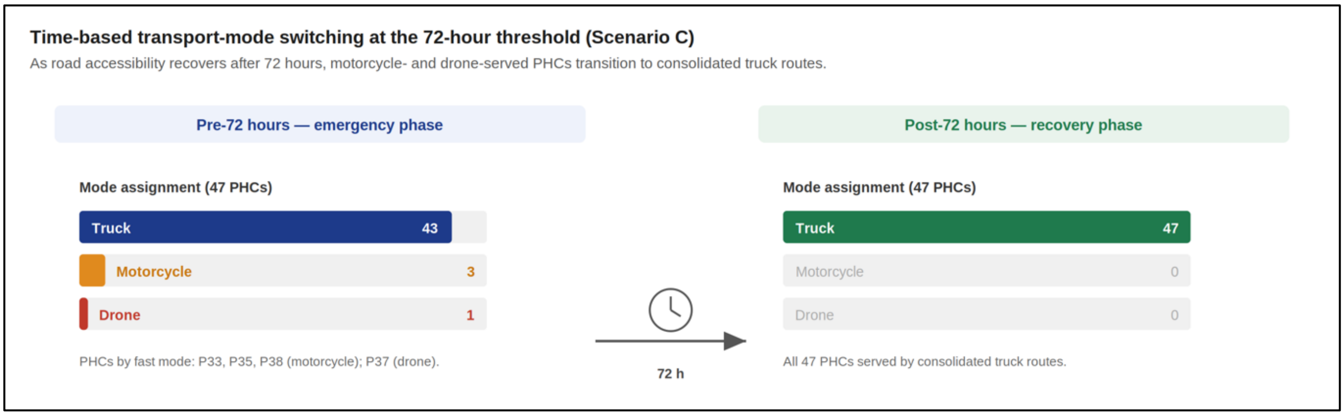

Figure 6 Mode Transition Scheme

Table 6 Mode Switching of the Four Transitioning PHCs at the 72-Hour Threshold

PHC	Pre-72 H Mode	Post-72 H Mode
P33	Motorcycle	→ Truck
P35	Motorcycle	→ Truck
P38	Motorcycle	→ Truck
P37	Drone	→ Truck

Table 7 Highest-Volume Consolidated Truck Routes over the 3-Month Horizon

Route	Service sequence	Stops	Trips
R017	P24-P36-P45	3	80
R019	P29-P32-P33-P35	4	75
R021	P37-P39-P40-P41	4	73
R016	P20-P22-P23-P34	4	69

Note: 11 multi-stop and 13 single-stop truck routes operate after the transition.

This finding aligns with the established humanitarian-logistics principle that the first 72 hours of disaster response prioritise speed and responsiveness over strict cost minimisation (United Nations Office for the Coordination of Humanitarian Affairs [UNOCHA], 2017; Feng & Wang, 2003), deliberately accepting a degree of operational redundancy— such as a higher number of direct, single-destination trips—while transportation infrastructure remains compromised. As the emergency phase transitions to recovery and road accessibility improves, the strategy shifts toward efficiency through consolidation. The two-phase structure of Scenario C, in which the route count expands during the emergency phase and consolidates thereafter, is therefore aligned with established phased-response frameworks that distinguish a responsiveness-oriented relief phase from an efficiency-oriented recovery phase (Wohlgemuth *et al.,* 2012), reflecting a deliberate, theoretically grounded trade-off rather than a modelling artefact.

5.1.6 Time-Based Mode Switching

A key contribution is time-dependent mode switching (Figure 6). In Scenario C, most PHCs are already served by truck during the first 72 hours, while a small number of access-constrained PHCs rely on motorcycles and drones under infrastructure constraints; after this period, these too switch to truck as roads recover—reflecting real disaster response, where early phases prioritise speed and access and later phases emphasise cost. Multi-modal routes (motorcycle–truck, drone–truck) further show the system's adaptivity. Unlike studies assuming static modes, this offers a more realistic representation of post-disaster operations.

This reflects the dynamic nature of post-disaster logistics: routing must adapt over time while coordinating multiple modes (Huang *et al.,* 2026). The proposed model reflects this perspective by enabling adaptive and coordinated distribution across different operational phases, thereby capturing both temporal variability and multimodal integration in post-disaster environments.

The spatial counterpart is Figure 7, mapping Scenario C's two-phase network. Panel (a) shows the pre-72-hour phase, where four access-constrained PHCs use fast modes (motorcycle: P33, P35, P38; drone: P37), giving 23 routes; panel (b) shows the post-72-hour phase, where these switch to truck and the network reverts to Scenario B's 24-route consolidated structure. The figure makes explicit that Scenario C's route structure is phase-dependent and that the extra saving comes from early-phase mode substitution, not changes to the route set.

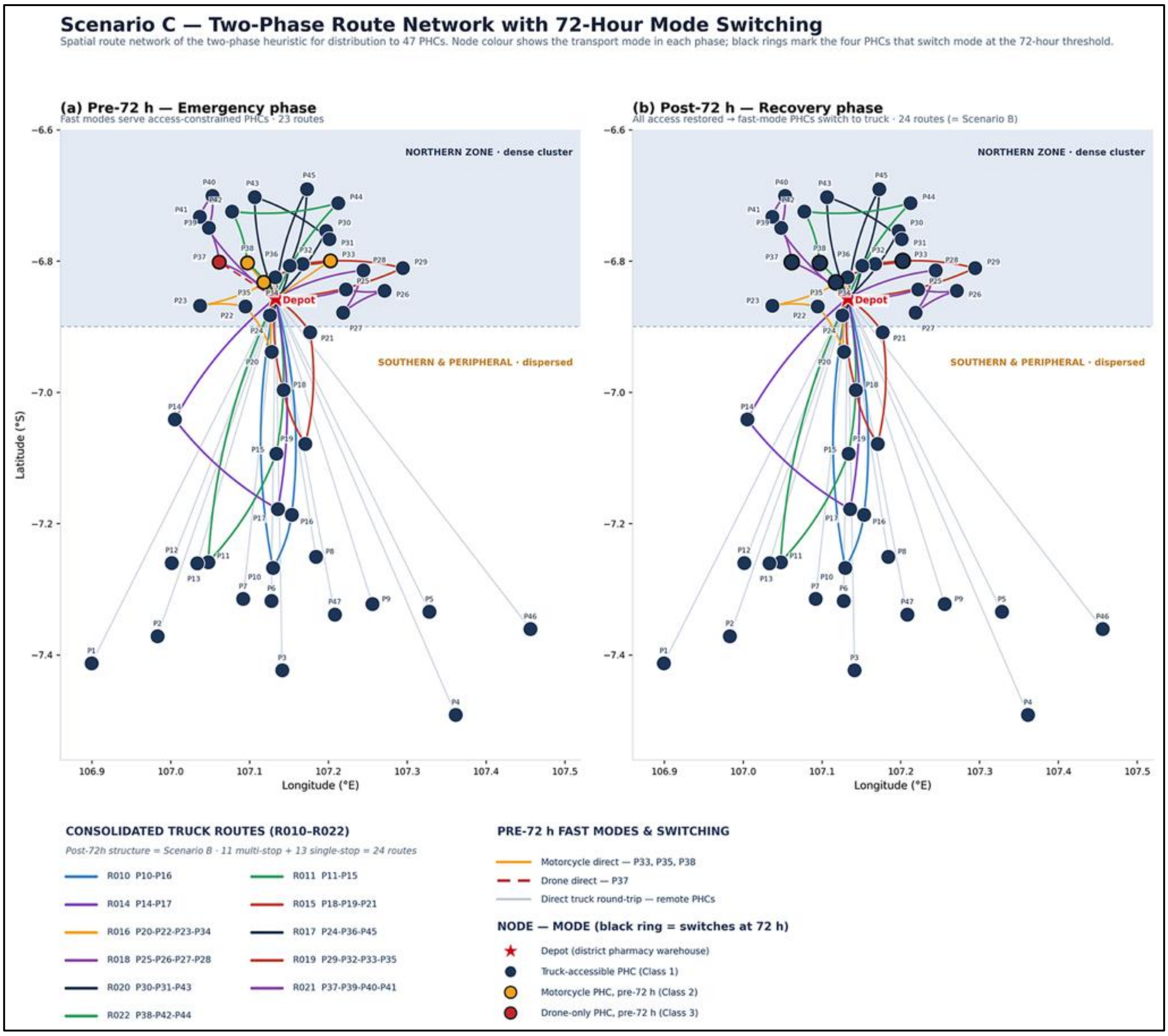

Figure 7 Two-Phase Route Network of Scenario C with 72-Hour Mode Switching

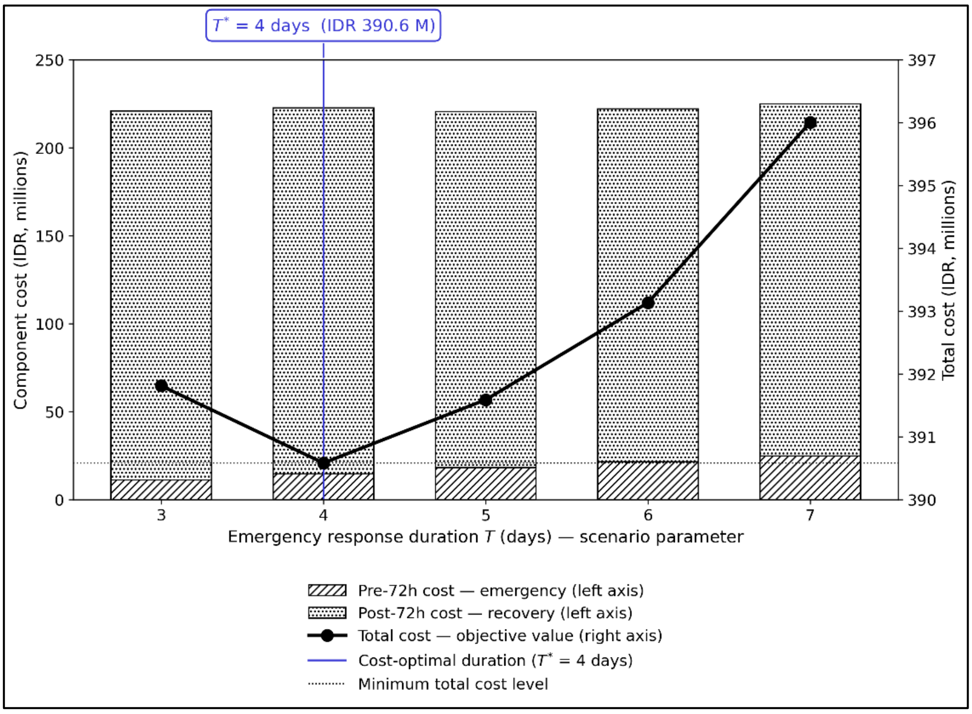

Figure 8 Sensitivity Analysis of Emergency Response Duration

5.1.7 Sensitivity Analysis of Emergency Duration

Emergency duration's impact on total cost is shown in Figure 8. A sensitivity analysis varied the duration from 3 to 7 days, solving the model independently for each.

Total cost follows a U-shape, falling from IDR 391,811,960 at 3 days to a minimum of IDR 390,583,200 at 4 days, then rising to IDR 396,005,711 at 7 days. This reflects a trade-off: longer emergency durations increase reliance on costly rapid modes, while shorter durations limit consolidation benefits. The optimal duration aligns with Balcik and Beamon (2008) on the speed–efficiency trade-off in humanitarian logistics.

The emergency response duration (3–7 days), denoted T*, is an exogenous parameter varied one value at a time, not a decision variable; for each fixed T* the model is solved independently and the heuristic total cost is recorded. The U-shape arises from two opposing components. As T* lengthens, the pre-72-hour cost rises because the system relies longer on fast but costly modes (the "speed" end), whereas the post-72-hour cost falls as a larger share of demand is eventually served by cheaper consolidated trucks (the "efficiency" end). Below the optimum, extending the emergency phase lowers total cost because the post-phase saving outweighs the pre-phase increase; beyond four days, the rising pre-72-hour cost dominates and total cost increases. The minimum at four days is therefore the point where the marginal pre-phase increase equals the marginal post-phase saving—the same transportation–overtime trade-off described in Section 4.1.4, now seen through the duration parameter. In Figure 8, the horizontal axis denotes the parameter T* (in days); the left vertical axis denotes the stacked pre-72-hour and post-72-hour cost components (IDR); the right vertical axis denotes the heuristic-based total cost (IDR); the dashed lines denote the linear trends of the two cost components (pre-72-hour rising, post-72-hour falling); and the circled marker denotes the optimal duration at T* = 4 days.

5.1.8 Model Validation and Implications

The model was validated through computational optimisation using the Gurobi solver, which was executed until the optimality gap reached 0%, indicating that the obtained solution satisfies the numerical optimality criteria of mixed-integer linear programming (MILP). In addition to solver-based validation, the model was evaluated using a scenario-based validation approach, consistent with established recommendations in simulation and optimisation studies (Sargent, 2013). The results demonstrate the optimisation scenario's responsiveness to strategic changes—reflected in the route reduction and cost saving reported in Section 5.1.2—thereby supporting its structural validity.

The heuristic approach produces solutions close to the optimal results while better capturing real-world operational constraints such as time-dependent accessibility and multimodal flexibility. Benchmarking the heuristic against the exact solver solution thus provides external validation through a reference solution, reinforcing the model's applicability for pharmaceutical logistics optimisation (Law, 2015).

The division of operations into pre-72-hour and post-72-hour phases aligns with widely recognised emergency-response practices in humanitarian logistics (UNOCHA, 2017), enhancing the model's practical relevance. During the emergency phase, the distribution cost amounts to IDR 10,296,273 for 69 priority packages, whereas the post-emergency phase yields 24 consolidated routes at a total cost of IDR 210,322,687. The service level, defined as the proportion of total pharmaceutical demand successfully delivered, reaches 100% in all three scenarios, each delivering the full 550 packages to all 47 PHCs (Table 4). For Scenario C, the 550 packages are fulfilled across both phases (69 in the pre-72-hour phase and 481 in the post-72-hour phase), so the 100% service level is preserved while distribution cost is minimised. This outcome is guaranteed by the constraint set, since full demand satisfaction at every PHC is imposed as a hard constraint in all three models (Equation 12), making the 100% service level a feasibility requirement rather than an emergent result.

Overall, the validation results demonstrate that the model is consistent across scenarios, adheres to operational logic, achieves substantial cost reductions, produces results comparable to those of exact optimisation solvers, and adapts effectively to emergency time constraints. Based on the validation criteria proposed in the literature, the model can therefore be considered operationally and methodologically valid and suitable for simulation-based decision support in post-disaster pharmaceutical logistics planning (Sargent, 2013; Law, 2015)

5.2 Strengths and Limitations of the Research

The study's strengths are threefold: it integrates heterogeneous VRP modelling, time-based mode switching, and overtime penalties in a unified framework; its application to the 2022 Cianjur Earthquake enhances external validity; and its sensitivity analysis of emergency duration provides novel insight into the speed–cost trade-off rarely quantified in disaster pharmaceutical logistics.

However, several limitations should be noted. Transportation mode selection is based on pre-disaster risk maps and does not fully capture the dynamic evolution of infrastructure conditions, where road recovery rates may vary across regions (Hsieh & Feng, 2018). The model also does not yet incorporate real-time GIS data, which could improve responsiveness under rapidly changing conditions, although its structure is inherently compatible with such integration and thus provides a foundation for future dynamic, real-time decision-support systems in disaster logistics. Despite these limitations, the proposed approach contributes to the advancement of efficient, adaptive, and data-driven pharmaceutical logistics in disaster contexts.

6. CONCLUSION

This study confirms the model improves route efficiency and significantly reduces distribution costs. Relative to baseline, route and mode optimisation cut total cost by 5.89%, while the integrated heuristic with adaptive mode switching achieved up to 8.89% reduction without compromising 100% service coverage. During the critical pre-72-hour phase, the model prioritised affected areas with few routes and minimal cost. Sensitivity analysis indicates a four-day emergency duration is most cost-efficient before full transition to trucks. These findings demonstrate the value of combining route optimisation, multimodal transport, and adaptive mode switching in disaster pharmaceutical logistics.

ACKNOWLEDGEMENTS

The authors gratefully acknowledge the relevant district health authority and the national meteorology and geophysics agency for providing data and field information that supported the development of this research model.

CONFLICTS OF INTEREST

The authors declare that they have no financial or personal relationship(s) that may have inappropriately influenced them in writing this article.

AUTHOR CONTRIBUTIONS

Author 1: Conceptualization, Methodology, Data curation, Writing–original draft, Writing–review & editing.
Author 2: Conceptualization, Methodology, Investigation, Supervision, Validation, Writing–review & editing.
Author 3: Conceptualization, Validation, Supervision, Writing–review & editing.
Author 4: Conceptualization, Supervision, Validation, Writing–review & editing.
Author 5: Software, Formal analysis, Visualization.

ETHICS STATEMENT

This study draws on secondary and aggregated data (road-network conditions, healthcare-facility demand, vehicle parameters, and published hazard zoning) and does not involve human participants, identifiable personal data, or animals. Ethical approval was therefore not required for the distribution-modelling component reported here.

USE OF AI TOOLS

The authors used a generative AI assistant to support language editing, figure preparation, and consistency checking. All analytical results, modelling decisions, and interpretations are the authors' own, and the authors take full responsibility for the content of the manuscript.

DATA AVAILABILITY STATEMENTS

The data supporting the findings of this study may be requested from the corresponding author.

REFERENCES

Balcik, B., & Beamon, B. M. (2008). Facility location in humanitarian relief. *International Journal of Logistics Research and Applications, 11*(2), 101–121. https://doi.org/10.1080/13675560701561789

Blagojević, N., Didier, M., & Stojadinović, B. (2022). Simulating the role of transportation infrastructure for community disaster recovery. *Proceedings of the Institution of Civil Engineers–Bridge Engineering, 175*(3), 150–159. https://doi.org/10.1680/jbren.21.00018

Bobdey, S. (2012). Strategic national pharmaceutical stockpile: A concept for optimization of medical resources during disasters. *Indian Journal of Community Medicine, 37(*3), 191. https://doi.org/10.4103/0970-0218.99929

Chen, D., Fang, X., Li, Y., Ni, S., Zhang, Q., & Sang, C. K. (2022). Three-level multimodal transportation network for cross-regional emergency resources dispatch under demand and route reliability. *Reliability Engineering & System Safety, 222*, 108461. https://doi.org/10.1016/j.ress.2022.108461

Cheng, J., Zhou, Y., Wu, C., & Li, Z. (2024). Collaborative truck–drone–motorcycle delivery of emergency supplies for mountain wildfire suppression. *Computers & Industrial Engineering, 196*, 110468. https://doi.org/10.1016/j.cie.2024.110468

Clarke, G., & Wright, J. W. (1964). Scheduling of vehicles from a central depot to a number of delivery points. *Operations Research, 12*(4), 568–581. https://doi.org/10.1287/opre.12.4.568

Dukkanci, O., Koberstein, A., & Kara, B. Y. (2023). Drones for relief logistics under uncertainty after an earthquake. *European Journal of Operational Research, 310*(1), 117–132. https://doi.org/10.1016/j.ejor.2023.02.038

Escribano Macias, J., Goldbeck, N., Hsu, P.-Y., Angeloudis, P., & Ochieng, W. (2020). Endogenous stochastic optimisation for relief distribution assisted with unmanned aerial vehicles. *OR Spectrum, 42*(4), 1089–1125. https://doi.org/10.1007/s00291- 020-00602-z

Feng, C.-M., & Wang, T.-C. (2003). Highway emergency rehabilitation scheduling in post-earthquake 72 hours. *Journal of the 5th Eastern Asia Society for Transportation Studies, 5*.

Golden, B., Raghavan, S., & Wasil, E. (2008). *The vehicle routing problem: Latest advances and new challenges*. Springer. https://doi.org/10.1007/978-0-387-77778-8

Goodarzian, F., Hosseini-Nasab, H., Muñuzuri, J., & Fakhrzad, M.-B. (2020). A multi-objective pharmaceutical supply chain network based on a robust fuzzy model: A comparison of meta-heuristics. *Applied Soft Computing, 92*, 106331. https://doi.org/10.1016/j.asoc.2020.106331

Guha-Sapir, D., & Vos, F. (2011). Earthquakes, an epidemiological perspective on patterns and trends. In R. Spence, E. So, & C. Scawthorn (Eds.), *Human Casualties in Earthquakes* (Vol. 29, pp. 13–24). Springer. https://doi.org/10.1007/978-90-481-9455-1_2

Holguín-Veras, J., Pérez, N., Jaller, M., Wassenhove, L. N. V., & Aros-Vera, F. (2013). On the appropriate objective function for post-disaster humanitarian logistics models. *Journal of Operations Management, 31*(5), 262–280. https://doi.org/10.1016/j.jom.2013.06.002

Hsieh, C.-H., & Feng, C.-M. (2018). The highway resilience and vulnerability in Taiwan. *Transport Policy, 87*. https://doi.org/10.1016/j.tranpol.2018.08.010

Huang, Y., Cui, H., Lu, Y., & Sun, Y. (2026). Modeling a reliable intermodal routing problem for emergency materials in the early stage of post-disaster recovery under uncertainty of demand and capacity. *Applied System Innovation, 9*(2), 27. https://doi.org/10.3390/asi9020027

Ikaditya, L., Zazuli, Z., Hidayat, Y. A., & Adnyana, I. K. (2025). The development of a standardized earthquake emergency health kit using combined ABC-VED classification and considering local wisdom for disaster response in Indonesia. *Disaster and Emergency Medicine Journal, 10*(3). 152–162. https://doi.org/10.5603/demj.104412

Khanmohammadi, M., Eshraghi, M., Sayadi, S., & Mashhadinezhad, M. G. (2023). Post-earthquake seismic assessment of residential buildings following Sarpol-e Zahab (Iran) earthquake (Mw7.3) part 1: Damage types and damage states. *Soil Dynamics and Earthquake Engineering, 173*, 108121. https://doi.org/10.1016/j.soildyn.2023.108121

Laporte, G. (2009). Fifty Years of Vehicle Routing. *Transportation Science, 43*(4), 408–416. https://doi.org/10.1287/trsc.1090.0301

Law, A. M. (2015). *Simulation modeling and analysis* (5th Ed.). McGraw-Hill.

Luo, H., Dridi, M., & Grunder, O. (2023). A branch-price-and-cut algorithm for a time-dependent green vehicle routing problem with the consideration of traffic congestion. *Computers & Industrial Engineering, 177*, 109093. https://doi.org/10.1016/j.cie.2023.109093

Ma, W., Lin, S., Ci, Y., & Li, R. (2024). Resilience evaluation and improvement of post-disaster multimodal transportation networks. *Transportation Research Part A: Policy and Practice, 189*, 104243. https://doi.org/10.1016/j.tra.2024.104243

Masmoudi, M. A., Mancini, S., Baldacci, R., & Kuo, Y.-H. (2022). Vehicle routing problems with drones equipped with multi-package payload compartments. *Transportation Research Part E: Logistics and Transportation Review, 164*, 102757. https://doi.org/10.1016/j.tre.2022.102757

Menares, F., Montero, E., Paredes-Belmar, G., & Bronfman, A. (2023). A bi-objective time-dependent vehicle routing problem with delivery failure probabilities. *Computers & Industrial Engineering, 185*, 109601. https://doi.org/10.1016/j.cie.2023.109601

Ministry of Public Works and Public Housing. (2022). *After the earthquake, the Puncak–Cianjur national road section is now passable*. https://binamarga.pu.go.id/index.php/berita/pasca-gempa-ruas-jalan-nasional-puncak-cianjur-sudah-bisa-dilalui

Ministry of Transportation RI. (2019). *Regulation of the Minister of Transportation of the Republic of Indonesia No. PM 60 of 2019 on the implementation of goods transportation by motor vehicles on roads.*

Mukherji, A., Ganapati, N. E., & Rahill, G. (2014). Expecting the unexpected: Field research in post-disaster settings. *Natural Hazards, 73*(2), 805–828. https://doi.org/10.1007/s11069-014-1105-8

Najafi, M., Eshghi, K., & Dullaert, W. (2013). A multi-objective robust optimization model for logistics planning in the earthquake response phase. *Transportation Research Part E: Logistics and Transportation Review, 49*(1), 217–249. https://doi.org/10.1016/j.tre.2012.09.001

Parker, E., & Maynard, V. (2015). *Humanitarian response to urban crises: A review of area-based approaches*. International Institute for Environment and Development (IIED). https://www.iied.org/10742iied

Pinzón, L. A., Hidalgo-Leiva, D. A., Alva, R. E., Mánica, M. A., & Pujades, L. G. (2023). Correlation between seismic intensity measures and engineering demand parameters of reinforced concrete frame buildings through nonlinear time history analysis. *Structures, 57*, 105276. https://doi.org/10.1016/j.istruc.2023.105276

Rahadian, F. (2020). *Feasibility analysis of commercial cargo unmanned aerial vehicle operations in Indonesia* [Undergraduate thesis]. Institut Teknologi Bandung.

Ramadhan, F., Irawan, C. A., Salhi, S., & Cai, Z. (2025). The truck traveling salesman problem with drone and boat for humanitarian relief distribution in flood disaster: Mathematical model and solution methods. *European Journal of Operational Research, 322*(1), 270–291. https://doi.org/10.1016/j.ejor.2024.10.022

Romero-Mancilla, M. S., Hernandez-Ruiz, K. E., & Huerta-Muñoz, D. L. (2024). A multiobjective mathematical model for a humanitarian logistics multimodal transportation problem. *Journal of Humanitarian Logistics and Supply Chain Management, 14*(3), 247–261. https://doi.org/10.1108/JHLSCM-01-2023-0004

Roque, P. J. C., Violanda, R. R., Bernido, C. C., & Soria, J. L. A. (2024). Earthquake occurrences in the Pacific Ring of Fire exhibit a collective stochastic memory for magnitudes, depths, and relative distances of events. *Physica A: Statistical Mechanics and Its Applications, 637*, 129569. https://doi.org/10.1016/j.physa.2024.129569

Sakarya, A., Akın, O., & Kılıç, A. (2024). Investigating the damage from the February 6, 2023 earthquakes in terms of building characteristics in the Antakya and Defne districts of Hatay province. *International Journal of Disaster Risk Reduction, 112*, 104783. https://doi.org/10.1016/j.ijdrr.2024.104783

Sakuraba, C. S., Santos, A. C., Prins, C., Bouillot, L., Durand, A., & Allenbach, B. (2016). Road network emergency accessibility planning after a major earthquake. *EURO Journal on Computational Optimization, 4*(3), 381–402. https://doi.org/10.1007/s13675-016-0070-2

Sargent, R. G. (2013). Verification and validation of simulation models. *Journal of Simulation, 7*(1), 12–24. https://doi.org/10.1057/jos.2012.20

Shabaninejad, H., Mehralian, G., Rashidian, A., Baratimarnani, A., & Rasekh, H. R. (2014). Identifying and prioritizing industry-level competitiveness factors: Evidence from pharmaceutical market. *DARU Journal of Pharmaceutical Sciences, 22*(1), 35. https://doi.org/10.1186/2008-2231-22-35

Shi, Y., Yang, J., Han, Q., Song, H., & Guo, H. (2024). Optimal decision-making of post-disaster emergency material scheduling based on helicopter–truck–drone collaboration. *Omega, 127*, 103104. https://doi.org/10.1016/j.omega.2024.103104

Sianturi, L. S. A. D. (2023). *Optimization model for motorcycle utilization in last-mile distribution in urban areas* [Master's thesis]. Institut Teknologi Bandung.

United Nations Office for the Coordination of Humanitarian Affairs. (2017). *5 essentials for the first 72 hours of disaster response.* https://www.unocha.org/publications/report/world/5-essentials-first-72-hours-disaster-response

Van Berlaer, G., Staes, T., Danschutter, D., Ackermans, R., Zannini, S., Rossi, G., Buyl, R., Gijs, G., Debacker, M., & Hubloue, I. (2017). Disaster preparedness and response improvement: Comparison of the 2010 Haiti earthquake-related diagnoses with baseline medical data. *European Journal of Emergency Medicine, 24*(5), 382–388. https://doi.org/10.1097/MEJ.0000000000000387

Weng, X., She, W., Fan, H., Zhang, J., & Yun, L. (2024). Multi-depot vehicle routing problem with drones in emergency logistics. *Cluster Computing, 28*. https://doi.org/10.1007/s10586-024-04809-5

Wohlgemuth, S., Oloruntoba, R., & Clausen, U. (2012). Dynamic vehicle routing with anticipation in disaster relief. Socio-Economic *Planning Sciences, 46*(4), 261–271. https://doi.org/10.1016/j.seps.2012.06.001

Zhao, S., Jiang, M., Kuang, H., & Wan, M. (2024). Decision-making optimization for post-disaster restoration of multimodal transport networks in terms of resilience. *Journal of Transport & Health, 39*, 101928. https://doi.org/10.1016/j.jth.2024.101928

Lingga Ikaditya is a pharmacist and academic, currently a Ph.D. candidate at Institut Teknologi Bandung (ITB), Indonesia, whose research focuses on the optimisation of pharmaceutical logistics in disaster contexts. His work is grounded in operations research, employing mixed-integer linear programming and advanced heterogeneous vehicle routing formulations to design efficient, time-sensitive, and resilient medical supply distribution systems under infrastructure and accessibility constraints. He integrates multi-modal transportation and time-dependent decision frameworks to capture the dynamic nature of post-disaster logistics. His research contributes to the development of robust decision-support models for humanitarian supply chains, with particular application to earthquake response in Indonesia.

Yosi Agustina Hidayat is a senior academic in Industrial Engineering at Institut Teknologi Bandung (ITB), Indonesia, with expertise in supply chain management, logistics systems, and decision analysis. She obtained her doctoral degree from Hiroshima University, Japan, and her research focuses on the optimisation and integration of supply chain systems using quantitative modelling, including multi-criteria decision-making and system-based approaches. Her work contributes to improving supply chain efficiency, coordination, and resilience across industrial and applied contexts.

Zulfan Zazuli is a pharmacist and academic at the School of Pharmacy, Institut Teknologi Bandung (ITB), Indonesia, with expertise in clinical pharmacy, pharmacogenomics, and evidence-based therapeutics. He obtained his Ph.D. from the University of Amsterdam, with research focusing on optimising drug safety and therapeutic outcomes through precision medicine approaches. His work provides a strong clinical and pharmacological foundation for healthcare decision-making, contributing to the integration of clinical evidence into pharmaceutical supply chain design and optimisation. His research supports the alignment of medical necessity, drug prioritisation, and patient safety within data-driven and resilient healthcare logistics systems.

I Ketut Adnyana is a professor of pharmacology at the School of Pharmacy, Institut Teknologi Bandung (ITB), Indonesia, specialising in natural product pharmacology, pharmacotherapy, and drug development. He obtained his Ph.D. from Toyama Medical and Pharmaceutical University, Japan, and has extensive experience in pharmacological research, particularly in metabolic disorders, inflammation, and neuroprotection. His work provides a strong pharmacological and clinical foundation for evidence-based decision-making, contributing to the integration of therapeutic efficacy, drug safety, and prioritisation into the design of resilient and responsive pharmaceutical supply chains in healthcare and disaster settings.

Zulfian Muhammad Furqon is an industrial engineering graduate with a focus on industrial systems and value chain analysis. His work is oriented towards supply chain optimisation and process improvement, with an emphasis on operational efficiency and quality management. He contributes to the application of data-driven and system-based approaches in logistics and supply chain contexts, supporting the development of efficient and scalable distribution systems.